

Compact Tactile Display for Fingertips with Multiple Vibrotactile Actuator and Thermoelectric Module

Gi-Hun Yang, Tae-Heon Yang, Seung-Chan Kim, Dong-Soo Kwon, and Sung-Chul Kang

Abstract—In this paper, a compact tactile display which consists of multiple vibrotactile actuators with 4-different vibrotactile unbalanced masses and a peltier thermoelectric module is proposed. By stimulating 2 different sensory channels including mechano-receptors and thermo-receptor simultaneously, surface texture and material composition can be displayed using the implemented device. 3 experiments were conducted for the performance evaluation of the proposed device through discriminating various patterned textures. Experimental results show that the developed device can be used to display surface texture and temperature together and suggest the possibility of implementing a small-sized, multi-fingered tactile display device.

I. INTRODUCTION

Until now, there have been lots of attempts to display realistic touch senses in the virtual environment. L. Winfield et al.[1] used piezoelectric crystal stack in their fabrication to build an ultrasonically vibrating plate that creates various textures by controlling the coefficient of friction. Q. Wang et al.[2] developed a tactile transducer system which consists of 6x10 piezo bimorph actuator arrays to generate a relatively large lateral skin deformation by adjusting the cantilever mechanics. T. Iwamoto et al.[3] proposed the 2-D scanning tactile display composed of ultrasound linear arrays. Y. Makino et al.[4] suggested a large-area tactile display actuated by suction pressure based on the tactile illusion that pulling a skin causes a sensation of pushing. C. R. Wagner et al.[5] used the servo motor to operate an array of mechanical pins which can generate reasonable frequency, amplitude, and high force capabilities. In the recent work, especially, one of the most prominent tactile display is attempted by Kyung et al.[6] using the

piezoelectric bimorphs. In their system, 6x5 pin-arrays are actuated by 30 piezoelectric bimorphs that have great advantages on the wide range of amplitudes and frequencies and the relatively high blocking force providing high performance over any desired patterned texture. In spite of a considerable progress, it requires high voltage to actuate the system, so it is hard to be miniaturized due to the massive controller system. One of the choices available to the tactile display was a vibrotactile motor. A. Kron et al.[7] used a vibration motor on the miniaturized tactile display for multi-fingered tactile feedback. However, there was a limitation on using one vibration motor that is coupled between frequency and amplitude. To compensate this limitation, we utilized four vibration motors with different unbalanced masses. It can demonstrate the wide range of amplitude on each frequency, and also increases the resolution on each motor making a user discriminate the moving direction and ridges on 2D surface. To achieve a holistic tactile feedback[16], it is insufficient to stimulate only cutaneous channels because human can sense the material properties through a temperature variation when touching an object. Because human fingers are often warmer than the room temperature objects in the environment, thermal perception occurs based on a combination of thermal conductivity, thermal capacity, and temperature. We can infer the material composition as well as temperature difference during thermal perception. Thermal feedback is relatively new research area[13], but Jones[14][15], Caldwell[10], Ino[11] and Bergamasco[12] have studied the thermal perception and feedback devices, researching experimental approaches and thermophysical factors that affect our ability to determine the material properties of an object. However, for cutaneous feedback devices, research on thermal feedback is nascent, particularly in terms of combining the two main components of tactile display. In this paper, we introduce the compact tactile display to stimulate both cutaneous and thermal channel.

In section 2, the characteristics of the vibration motors with different unbalanced mass were analyzed to verify the possibilities to decouple the frequency and amplitude and stimulating two channels, Pacinian and Meissner, simultaneously by mixing vibrations. In section 3, hardware configuration of the proposed tactile display is depicted. In section 4, the procedure of the implemented vibrotactile rendering is explained. In section 5, the experimental evaluations are provided. In section 6, we discuss the

Manuscript received September 15, 2006. This work has been supported by 'TSI-ITE(Immersive Tangible Environment)(KIST)' and 'Development of Smart Haptic Interface Device(2004-S-30, Korea Ministry of Information and Communication)'

G. H. Yang T. H. Yang and S. C. Kim are with the Mechanical Engineering Department, Korea Advanced Institute of Science and Technology, 373-1 Guseong-dong, Yuseong-gu, Daejeon, 305-701, Korea(e-mail: yanggh;yangth;kimsc@robot.kaist.ac.kr).

D. S. Kwon is with Human-Robot Interaction Research Center, Korea Advanced Institute of Science and Technology, 373-1 Guseong-dong, Yuseong-gu, Daejeon, 305-701, Korea(corresponding author to provide phone:+82-42-869-3042; fax:+82-42-869-3095; e-mail: kwonds@kaist.ac.kr)

S. C. Kang is with Intelligent Robotics Research Center, Korea Institute of Science and Technology, Hawolgok-dong 39-1, Sungbuk-ku, Seoul 136-791, Korea (e-mail: kasch@kist.re.kr).

effectiveness of our developed tactile display system that stimulates tactile and thermal channels. For the future works, further tactile rendering and experimental plans are discussed.

II. THE CHARACTERISTICS OF THE VIBRATION MOTOR

An experiment was conducted to obtain the frequency and amplitude of the vibration motor according to the unbalance and input voltage.

A. Additional Unbalanced Mass

The commercial vibration motor generally has one type of unbalanced-mass, therefore it is hard to modulate the wide range of frequency and amplitude. The necessity leads us to fabricate the nine kinds of the additional unbalanced mass using RP(rapid prototyping), automatic construction method of physical objects using solid freeform fabrication, as shown in Fig. 1.

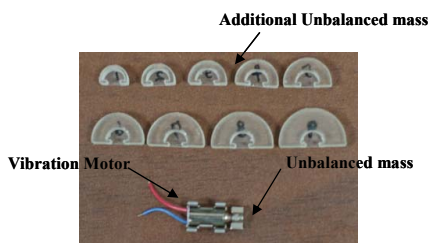


Fig. 1. Additional Unbalanced Mass

Inner Radius	Outer Radius	Unbalance(=me)
2.5mm	3.0mm	0.56g-mm
	3.5mm	0.62g-mm
	4.0mm	0.7g-mm
	4.5mm	0.81g-mm
	5.0mm	0.97g-mm
	5.5mm	1.14g-mm
	6.0mm	1.35g-mm
	6.5mm	1.6g-mm
7.0mm	1.89g-mm	

Table.1. Additional Unbalanced Mass Size & the Unbalance

While the inner radius of the additional unbalanced mass is same as the radius of the vibration motor's unbalanced mass, the outer radius of additional unbalanced mass is increased by 0.5mm each refer to Table. 1.

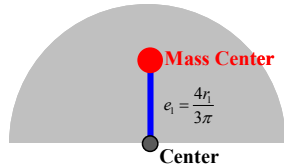


Fig.2. Mass Center & Eccentricity, e_2 of Unbalanced Mass

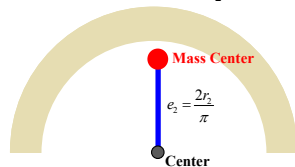


Fig.3. Mass Center & Eccentricity, e_2 of Additional Unbalanced Mass

The centrifugal force, $me\omega^2$ of vibration motor by the unbalanced mass consists of multiplication among the unbalanced mass, the eccentricity, e , and the square of frequency, $me\omega^2$. The total centrifugal force of vibration motor by the unbalanced and additional unbalanced mass is shown in (1)

$$\begin{aligned}
 me\omega^2 &= m_1e_1\omega^2 + m_2e_2\omega^2 \\
 &= \omega^2(m_1e_1 + m_2e_2) \\
 &= \omega^2\left(m_1\frac{4r_1}{3\pi} + m_2\frac{2r_2}{\pi}\right)
 \end{aligned}
 \tag{1}$$

The unbalances, me , obtained from equation (1) are displayed quantitatively in Table.1. The additional unbalanced masses of 4.0mm, 5.5mm, 7.0mm are attached to the new tactile display, as shown in Fig. 4.

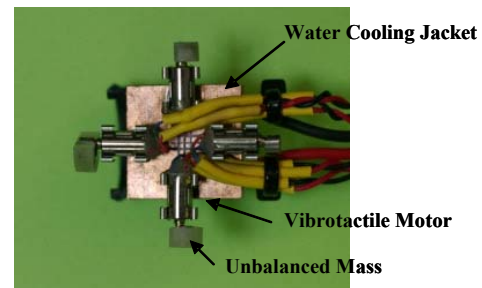


Fig.4. Tactile & Thermal Display

B. Experimental Setup

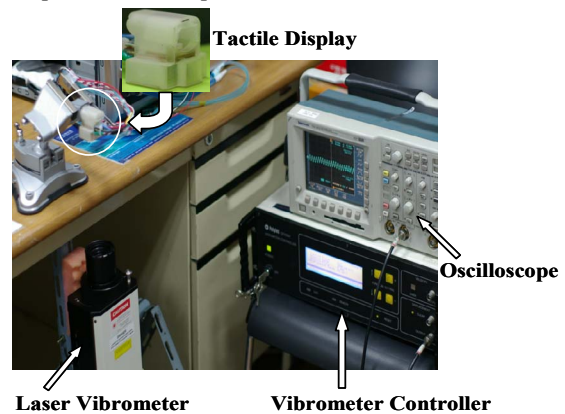


Fig.5. Tactile Display with Laser Vibrometer

To measure the frequency and the amplitude on the surface of our tactile display, we used the OFV-505 Sensor Head(Laser Vibrometer), OFV-5000 Vibrometer Controller, and Oscilloscope, as shown in Fig. 5.

C. Result for one Motor

The motor without the additional unbalanced mass is indexed as the first, the second for 4mm, the third for 5.5mm, and the fourth for 7.0mm. The motors are driven with a motor power of 20%, 30%, 40%, 60%, 80%, and 100% respectively to measure the frequency and amplitude from our tactile display quantitatively.

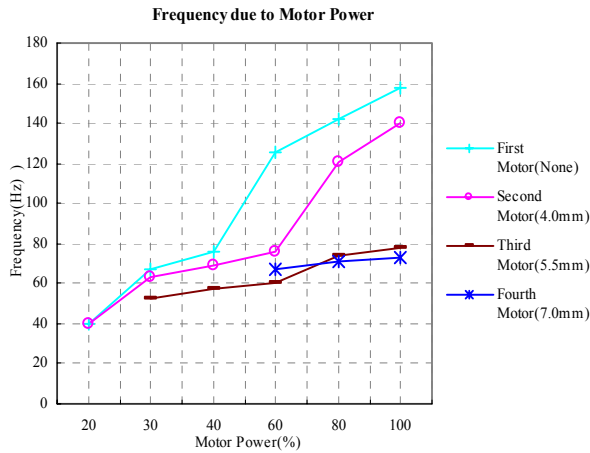


Fig.6. The result of the frequency from each vibration motor with the different unbalanced mass with the increase of the motor power

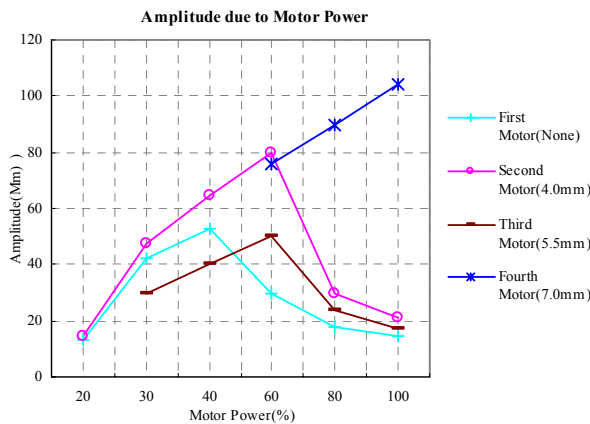


Fig.7. The result of the amplitude from each vibration motor with the different unbalanced mass with the increase of the motor power

As shown in Fig.6 and Fig.7, we obtained the frequency and amplitude resulted from each vibration motor with the different unbalanced mass according to the motor power. The frequency generally increased with increasing motor power. However, the amplitude started to decrease after a specific point. Especially, it can be seen that the frequency and amplitude from same motor power have different values of amplitude according to the unbalance, *me*.

D. Result for two & four Motor

In the same condition with section 2-C, another experiment was conducted to verify the frequency and amplitude resulted from two and four vibration motors with the different unbalanced mass according to the motor power. First, we measured the frequency and amplitude on the combination of the first and fourth motor with 4.0mm and 7.0mm unbalanced mass with respect to the motor power. In this way, with the combination of the second(4.0mm) and third(5.5mm), the first(none) and third(5.5mm), the second(4.0mm) and fourth(7.0mm), and all motors were experimented.

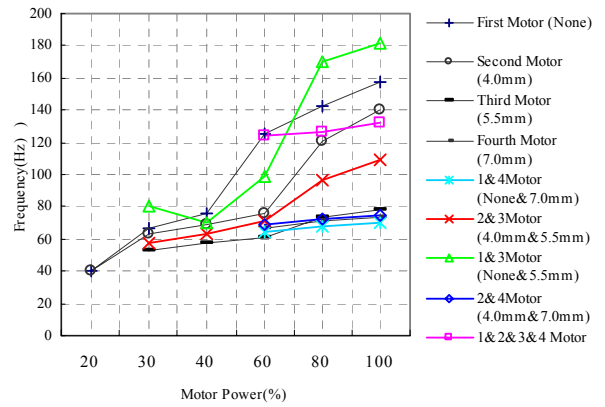


Fig.8. The result of the frequency from two and four vibration motors with the different unbalanced mass with the increase of the motor power

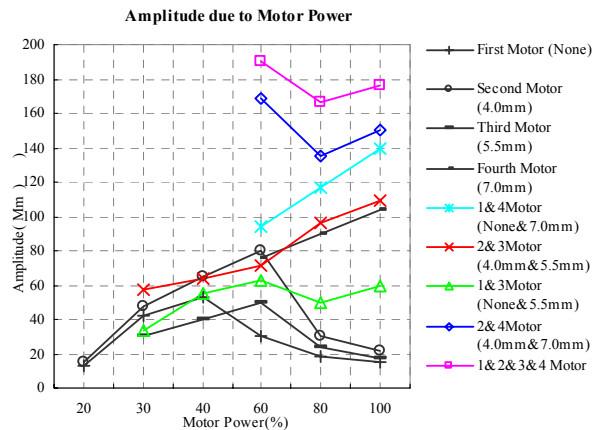


Fig.9. The result of the amplitude from two and four vibration motors of the different unbalanced mass with the increase of the motor power

As shown in Fig.8 and Fig.9, the combination of two and four motors generated the different frequency and amplitude on the same motor power. Therefore, we found the possibility that the tactile display actuated by motors with the four different unbalanced mass can modulate the frequency and amplitude on the range of $16(=2^4)$ combinations.

III. DESCRIPTION OF THE TACTILE DISPLAY SYSTEMS

A. Tactile Display Unit

In this section, we describe the overall structures and design specifications of the tactile & thermal display device

Design Specification

By considering of specification of the vibration motor and realistic sense of touch, we determined the following principal requirements for the tactile & thermal display device:

- A minimum displacement that is 5 times more than the threshold value of the nerve system.
- Various combinations of frequency and amplitude.

- Sufficient ability to absorb or emit heat on 5°C/s for cooling and 10°C/s for heating with achievable range of 18–45°C so that the different thermophysical properties of objects can be displayed.

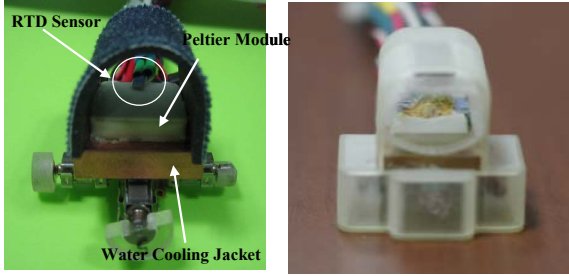


Fig.10. Tactile and Thermal Display Unit & Prototype

Implementation of Vibrotactile Display Part

We have designed and fabricated tactile & thermal display device based on the derived requirement as shown in Fig.10. The size of a cover is 38.5mm×31.7mm and its height is 38.5mm. The size of a motor is R2.5mm and the length is 11mm. The driving voltage of a motor is 0-5 V and the maximum speed of a motor is 216Hz. The distance between motors on the water cooling jacket is 11mm each. We fabricated a 3mm × 8mm × 2mm cantilever beam as a supporter of motors to increase the amplitude and resolution rate of vibration. The additional unbalanced mass is attached to vibration motor, where the radius of the additional mass is R4.0mm, R5.5mm, and R7.0mm each as shown in Fig.10.

B. Thermal Display Part.

A peltier thermoelectric module is used as a heat pump because of its fast response and controllability. Since the performance of a peltier thermoelectric module depends on cooling the heat generating side of the module, we designed a miniaturized water cooling jacket that is attached to the heat generation side to increase performance as shown in Fig.10. The size of the peltier is 15mm×15mm and the thickness is 3.8mm. The size of the cooling jacket is 20mm×20mm and the thickness is 5mm. A small size RTD for measuring temperature is attached to the surface of the peltier thermoelectric module.

IV. VIBROTACTILE RENDERING

In this section, the implemented vibrotactile rendering algorithms will be described. The previous research shows that the common vibratory parameters are the amplitude, frequency, and damping[8]. From the explorative point of view, vibrotactile stimuli consists of tapping and stroking; tapping means that either fingertip collides with an object surface for a short time or it remains fixed on surface after a tap and stroking means that finger slides over an object surface[9]. The vibration feedback model developed from the tapping data is a decaying sinusoidal waveform[7][8].

$$Q(t) = A(v) e^{-Bt} \sin(2\pi\omega t) = k_{v,t} \cdot v_n e^{-Bt} \sin(2\pi\omega t) \quad (2)$$

The attack amplitude, $A(v)$, is the product $k_{v,t} \cdot v_n$, where $k_{v,t}$ is an object constant and v_n is a normal velocity to the object surface. The decay parameter, B , and frequency parameter, ω , remains constant and determined with respect to the type of material. On a patterned texture where, a series of grooves and ridges, we added a new concept to above equation during driving our new tactile display.

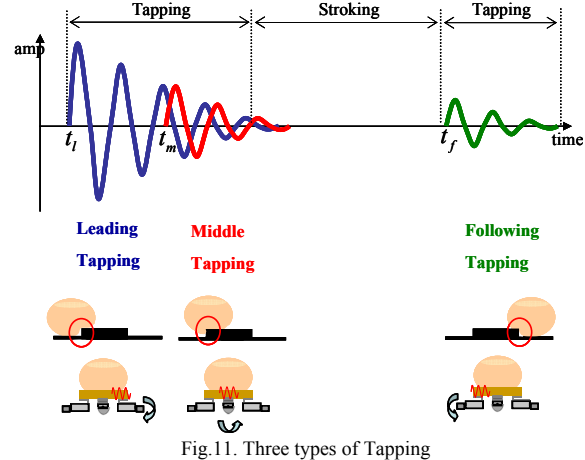


Fig.11. Three types of Tapping

As shown in Fig.11, the new tapping algorithm with the new tactile display is applied. Tapping can be divided into three types. When the fingertip encounters a patterned texture at first, the leading tapping occurs. In this moment, the right motor vibrates the right side of the fingertip on a relatively high motor power to generate large amplitude, as shown in Fig. 11. Right after the leading tapping, the middle tapping occurs. In the middle tapping, the top and bottom motor vibrates the middle area of the fingertip on a moderate motor power to generate the middle size of the amplitude, as shown in Fig. 11. At the end of the specific pattern, the following tapping happens. In the following tapping, the left motor vibrates the left side of the fingertip on a relatively low motor power to generate small amplitude, as shown in Fig.11. In order to make this algorithm more realistic, we considered the velocity of a mouse that human operates. Depending on the velocity of a mouse, the motor power on the tapping is increased or decreased. The velocity of a mouse is also divided into the horizontal and vertical one to make human operators discriminate the moving direction. Three types of tapping can be expressed as following equation.

$$Q_L = k_{t,v} \cdot v_{n,L} e^{-Bt} \sin(2\pi\omega t_L) \\ Q_M = k_{t,v} \cdot v_{n,L} e^{-Bt} \sin(2\pi\omega t_M) + k_{t,v} \cdot v_{n,M} e^{-Bt} \sin(2\pi\omega t_M) \\ = k_{t,v} e^{-Bt} \sin(2\pi\omega t_M) (v_{n,L} + v_{n,M}) \quad (3)$$

$$Q_F = k_{t,v} \cdot v_{n,F} e^{-Bt} \sin(2\pi\omega t_F)$$

Refer to (3), Q_L , Q_M , Q_F are the vibration feedback model for the leading, middle, and following tapping respectively. The stroking also can be expanded on the concept of leading, middle, and following.

V. PERFORMANCE EVALUATION AND RESULTS

In order to evaluate the performance and effectiveness of the tactile display, we performed 3 experimental tests for discriminating the patterned texture with various series of ridges.

A. EXPERIMENTAL METHOD

In order to utilize the proposed device as a quantitative tactile feedback device, the system should provide high resolution to discern the small object. So we made the patterns of ridges that have various width and interval in the first experiment. For the first experiment, we set the mouse moving speed so that 1024pixel is mapped with 11cm of user's movement. According to the conversion rate, we made the patterns of ridges with 2, 4, and 6mm- width, and 3, 6, and 9mm-interval for each width in virtual environment. Eventually, the nine vertical and horizontal patterns are made respectively, as shown in Fig. 12.

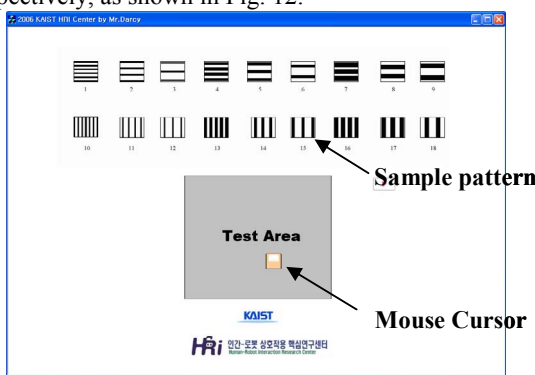


Fig.12. Virtual Environment for the 1st Experiment

The subjects were instructed to explore this virtual environment over the test area and to choose one of the sample patterns. Each sample was displayed randomly 4 times. 7 undergraduate students of KAIST(3 men, 4 women) were participated in this experiment.

In order to have the user to discern the amplitudes of ridges, the second experiment was conducted to discriminate 3 different levels of amplitude with vertical and horizontal patterns as shown in Fig. 13. 7 subjects were participated in this experiment.

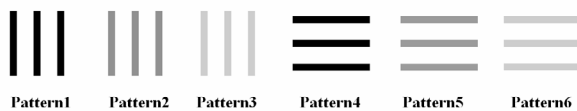


Fig.13. Patterns Used in the 2nd Experimental Procedure

One of the 6 patterns was randomly displayed to the subject and the subject was instructed to choose one of pattern after she/he stroked over the shadowed area freely. Each pattern was displayed randomly 6 times. Totally 36 trials were conducted for each subject and experimental procedure took about an hour.

To test the difference between cases when following tapping is included or not, the third experiment was conducted. 6 patterns were prepared with different width of ridges and the number of ridges as shown in Fig. 14.

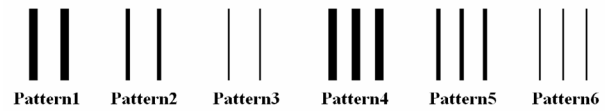


Fig.14. Patterns Used in the 3rd Experimental Procedure

One of the 6 patterns was randomly displayed to the subject and the subject was instructed to choose one of pattern after she/he stroked over the shadowed area freely. Each pattern was displayed randomly 6 times. Totally 36 trials were conducted for each subject and experimental procedure took about an hour. Experiment was conducted on 2 conditions, with and w/o following tapping.

For thermal display evaluation, 5 materials including urethane foam, wood, glass, stainless steel and copper were displayed same manner as Yang et al.[17] did. 10 subjects(5 men, 5 women) were participated in this experiment.

B. EXPERIMENTAL RESULTS AND DISSCUSION

The result obtained from the first experiment is presented in Table 2.

The Experimental type	The Discrimination Percentage of Correct Answers	
The vertical & horizontal patterns	93.75%	
The number of ridges on patterns	91.96%	
The width of ridges	2mm & 4mm	85.415%
	4mm & 6mm	68.75%
	6mm & 2mm	91.425%
The Interval between ridges	On width-2mm	75%
	On width -4mm	70.80%
	On width -6mm	64.58%

Table.2. Experimental Results

In the first experiment, the 18 alternative forced choice(18 AFC) method was applied, so chance rate is 11%, minimum correct answer rate is 64%. From this point of view, it is understood that subjects were reliably able to discriminate various patterns.

Results were categorized with following 4 conditions.

1. The percentage of correct discrimination on the horizontal and vertical patterns.
2. The percentage of correct discrimination on the number of ridges.
3. The percentage of correct discrimination on the width of 2, 4, 6mm ridges
4. The percentage of correct discrimination on the gap between ridges that has same ridge width.

In the first experiment, subjects used the sequence of scheduled event-leading tapping, middle tapping, and following tapping when discriminating direction of patterns (vertical or horizontal). When counting number of ridges, subjects used the characteristics of tapping, because it shows fast response and high values in the leading and following tapping. The temporal factor of vibrotactile information

would be used to discriminate the width of ridges with time interval between the leading and following tapping. Subjects have a tendency to use information of stroking when estimating the width of ridges. In the second experiment, percentage of correct answer was 86% and from confusion matrix of result, all subjects were able to discern perfectly horizontal and vertical ridges. From this result, 3 levels of ridges were reliably displayed using the developed device. In the third experiment, from result of condition with following tapping case, subjects were able to discriminate the width of ridges more reliably comparing to the case without following tapping (without: 73.8%, with: 91.7%). So the proposed algorithm was better for displaying widths of ridges in tactile rendering method using vibrotactile actuator.

As shown in Table 3, subjects were reliably able to identify which material is displayed using only thermal sensation. This result coincides with the real material's case [18].

Sample \ Answer	Urethane	Wood	Glass	SS	Copper
Urethane	77%	22%	2%	0%	0%
Wood	33%	52%	15%	0%	0%
Glass	10%	27%	52%	12%	0%
SS	2%	12%	37%	37%	13%
Copper	0%	2%	10%	43%	45%

Table 3. Confusion Matrix of 5 Material Displaying with Thermal Feedback

VI. CONCLUSION AND DISCUSSION

In this paper, we have proposed a compact tactile display device using 4 vibrotactile actuators with different unbalanced masses and a peltier thermoelectric module, and it shows the possibility of the compact wearable tactile display device. Frequency and amplitude are measured for each vibrotactile actuator and combinations of multiple vibrotactile actuators for quantitative vibrotactile feedback using Laser vibrometer. From result of measurements, multiple actuators have many advantages for displaying the various combinations of amplitude and frequency simultaneously. To display the thermophysical properties of 5 materials, thermal feedback unit that consists of peltier thermoelectric module, small-size water cooling jacket and thin film RTD were integrated with vibrotactile parts. 5 materials were displayed for thermal feedback. The subjects were reliably able to discriminate the 5 materials using the implemented device. A new modified tactile rendering algorithm based on A.M. Okamura's work were used and applied for tactile display method. 3 experimental evaluations using various 2D-patterns and results show that the proposed device can be used for displaying various 2D patterns reliably.

For future works, bio-mechanical analysis should be conducted for transmitting vibration to skin and mechano-receptors. Also multi-fingered vibrotactile feedback device will be implemented with proposed design concept.

REFERENCES

- [1] L. Winfield and T. Vose. "Virtual Texture Display using Ultrasonically Vibrating Plates," Laboratory for Intelligence Mechanical System. Northwestern Univ. MDS Study (unpublished) <http://lims.mech.northwestern.edu/projects/vfhd/>
- [2] Q. Wang and V. Hayward. "Compact, Portable, Modular, High-performance, Distributed Tactile Transducer Device Based on Lateral Skin Deformation," *2006 Symposium on Haptic Interfaces For Virtual Environment And Teleoperator Systems IEEE VR, Arlington, VA, 25-26 March 2006*, pp. 67-72.
- [3] T. Iwamoto and H. Shinoda. "Two-dimensional Scanning Tactile Display using Ultrasound Radiation Pressure," *Symposium on Haptic Interfaces for Virtual Environment and Teleoperator Systems 2006 March 25 - 26, Alexandria, Virginia, USA*
- [4] Y. Makino, N. Asamura and H. Shinoda. "A Whole Palm Tactile Display Using Suction Pressure," *Proceedings of the 2004 IEEE International Conference on Robotics & Automation, New Orleans, LA, April 2004*
- [5] C. R. Wagner, S. J. Lederman, and R. D. Howe, "Design and Performance of a Tactile Shape Display using RC Servomotors," Division of Engineering and Applied Sciences Harvard University
- [6] Kyung, K.U, Ahn, M., Kwon, D.S. and Srinivasan, M.A., "A Compact Broadband Tactile Display and Its Effectiveness in the display of Tactile Form," *Proc. of World Haptics: 2005, Pisa, Italy*, pp.18-20, 2005.
- [7] A. Kron and Gunther Schmidt, "Multi-fingered Tactile Feedback from Virtual and Remote Environments," *Proceedings of the 11th Symposium on Haptic Interfaces for Virtual Environment and Teleoperator Systems (HAPTICS'03) 0-7695-1890-7/03 \$17.00 © 2003 IEEE*
- [8] A.M. Okamura, J. T. Dennerlein, and R.D. Howe. "Vibration Feedback Models for Virtual Environment," *In Proc. of the IEEE International conference on Robotics and Automation*, pages 674-679, Leuven, Belgium, 1998.
- [9] S. Lederman and R. Klatzky. "Designing Haptic and Multimodal Interfaces : A Cognitive Scientist's Perspective," *In Proc. of the Workshop on Advances in Interactive Multimodal Telepresence Systems, pages 71-80, Munchen, March 2001*.
- [10] Caldwell, D.G.; Tsagarakis, N.; Wardle, A, "Mechano thermo and proprioceptor feedback for integrated haptic feedback, Proceedings of IEEE International Conference on Robotics and Automation, 1997. vol. 3 pp2491 -2496, 20-25 April 1997
- [11] Shuichi INO et al., "A Tactile Display for Presenting Quality of Materials by Changing the Temperature of Skin Surface," *Proceedings of IEEE International Workshop on Robot and Human Communication*, pp220-224, 1993
- [12] Massimo Bergamasco, A.A. Alessi and M. Calcara, "Thermal Feedback in Virtual Environments," *Presence, Vol.6, December 1997*, 617-629
- [13] Robert Howe, "Haptic Research – Tactile Display," the haptic community web site, april 3rd, 2002 <http://haptic.mech.northwestern.edu/TactileDisplay.html>
- [14] Lynette A. Jones and Michal Berris, "Material Discrimination and Thermal Perception," *Proceedings of the 11th symposium on Haptic Interfaces for Virtual Environment and Teleoperator Systems(HAPTICS'03)*, pp171-178
- [15] Lynette A. Jones and Michal Berris, "The Psychophysics of Temperature Perception and Thermal-Interface Design," *Proceedings of the 10th symposium on Haptic Interfaces for Virtual Environment and Teleoperator Systems(HAPTICS'02)*, pp137-142
- [16] Peter Kammermeier et al. "Display of Holistic Haptic Sensations by Combined Tactile and Kinesthetic Feedback," *Presence. Vol. 13 No.1 February 2004*, 1-15
- [17] Gi-Hun Yang, Ki-Uk Kyung, M.A.S Dong-Soo Kwon, "Quantitative Tactile Display Device with Pin-Array Type Tactile Feedback and Thermal Feedback", *Proc. Of the 2006 IEEE International Conf. on Robotics and Automation, Orlando, USA*, pp. 3917~3922, 2006
- [18] Hsin-Ni Ho and L.A. Jones, "Contribution of thermal cues to material discrimination and localization", *Perception & Psychophysics*, in press